Catalytic performance of electronic waste-derived gold nanoparticles for the reduction of *p*-nitrophenol

Michelle Y. Lau[a], David C. Young [b], Jack L.-Y. Chen [c,d,e], and Jonathan Sperry[a]

[a] *Centre for Green Chemical Science, University of Auckland, New Zealand*

[b] *Mint Innovation, 6 Hotunui Drive, Auckland, New Zealand*

[c] *Centre for Biomedical and Chemical Sciences, Auckland University of Technology, New Zealand*

[d] *The MacDiarmid Institute for Advanced Materials and Nanotechnology, New Zealand*

[e] *Department of Biotechnology, Chemistry and Pharmaceutical Sciences, Universita degli Studi di Siena, Italy*

[*] Corresponding author(s): mlau527@aucklanduni.ac.nz, j.sperry@auckland.ac.nz

Contents

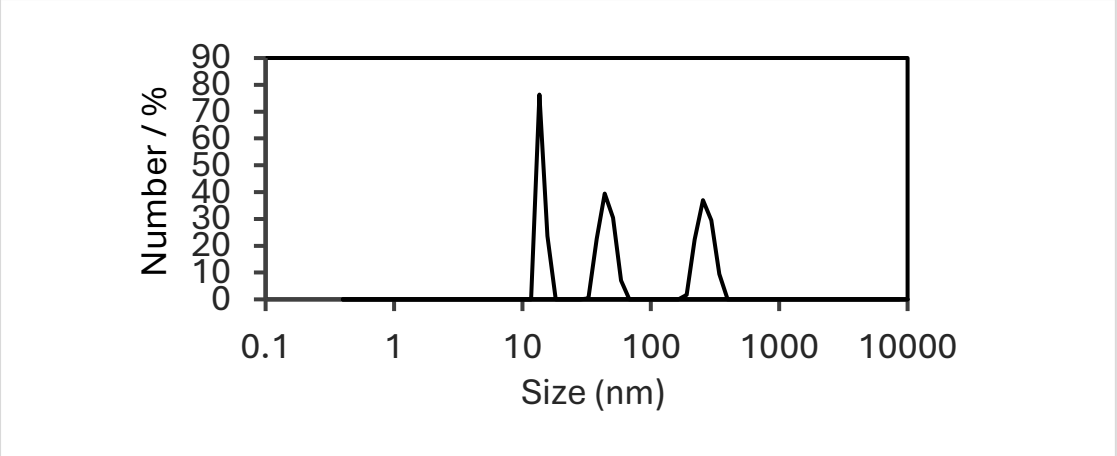

Figure S1. DLS measurement of trisodium citrate and free-base hydrazine hydrate in $AuCl_4^-$ model system at room temperature depicting size increase over the course of three triplicate readings

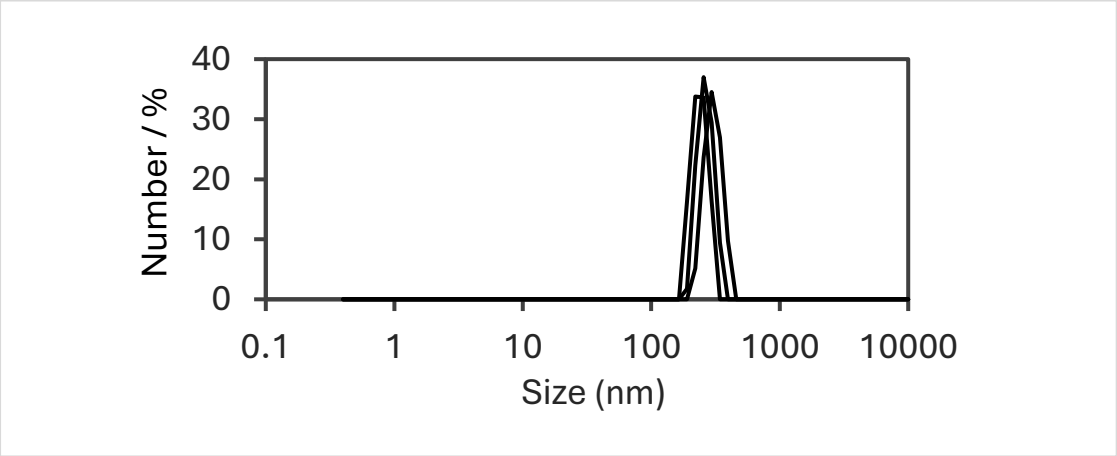

Figure S2. DLS measurement of trisodium citrate and free-base hydrazine hydrate in $AuCl_4^-$ model system at 70 ˚C depicting stable size over the course of three triplicate readings

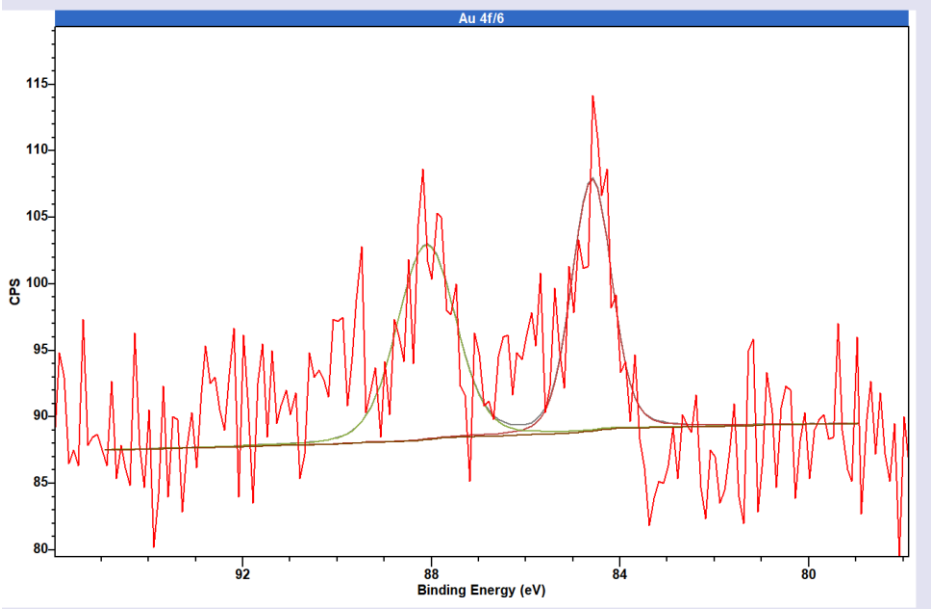

Figure S3. XPS spectra of AuNPs on polysulfide material signal showing the presence of Au (0) form, but with a much lower intensity in comparison to the XPS spectra of AuNPs on cellulose. Possibly indicative of Au(0) embedded in the porous structure of polysulfide material.

$AuCl_4^-$					
Temperature during catalyst synthesis					
Size range (nm)	10 ˚C	25 ˚C	40 ˚C	80 ˚C	100 ˚C
0 to 10	5%	10%	2%	9%	4%
10 to 20	51%	64%	53%	27%	43%
20 to 30	32%	14%	39%	39%	31%
30 to 40	8%	11%	4%	19%	18%
40 to 50	3%	1%	1%	3%	4%
50 plus	1%	-	-	-	0%

Table S1 Effect of temperature during catalyst synthesis on AuNPs size distribution for gold chloride model systems. Downward catalytic function as temperature during catalyst synthesis is attributed to the increase in size of resulting AuNPs generated at higher temperatures.

AuI_4^-					
	Temperature during catalyst synthesis				
Size range (nm)	10 ˚C	25 ˚C	40 ˚C	80 ˚C	90 ˚C
0 to 10	67%	72%	68%	70%	55%
10 to 20	26%	15%	29%	22%	36%
20 to 30	6%	5%	3%	3%	6%
30 to 40	1%	8%	-	4%	2%
40 to 50	1%	-	-	-	1%
50 plus	-	-	-	-	1%

Table S2 Effect of temperature during catalyst synthesis on AuNPs size distribution for gold chloride model systems. Negligible effect of temperature on the size of the resulting AuNPs, and hence a negligible effect of temperature during catalyst synthesis on the resulting AuNPs catalytic function.

AuNPs description		k_{app} [s^{-1}]	k_{app} [min^{-1}]	k_{app} [h^{-1}]	Calculated using	Reference
Colloidal	22 nm	0.0044	0.264	15.84	$\ln(A_t/A_0)$	1
	20 nm	0.0075	0.450	27.00		
	14 nm	0.0264	1.584	95.04		
Colloidal	4 nm	0.0208	1.247	74.82	$\ln(A_0/A_t)$	2
	16 nm	0.0061	0.363	21.78		
	40 nm	0.0039	0.234	14.04		
	117 nm	0.0296	1.776	106.56		
	134	0.0727	4.364	261.84		
Colloidal	8 to 35 nm	0.0054	0.322	19.31	$-\ln(C_t/C_0)$	3
Cellulose	N/A	0.0043	0.257	15.41		
	20 to 40 nm	0.0017	0.103	6.17		
Cellulose	14 nm	0.0045	0.268	16.09	$\ln(A_t/A_0)$	4
	16 nm	0.0037	0.222	13.32		
	26 nm	0.0021	0.128	7.67		
Cellulose	10 to 20 nm	0.0006	0.036	2.18	$\ln(A_t/A_0)$	5
		0.0007	0.041	2.43		
		0.0007	0.040	2.42		
		0.0005	0.031	1.84		
		0.0005	0.031	1.84		
Ionic cellulose	1 to 20 nm	0.0753	4.518	271.08	N/A	6
		0.0746	4.476	268.56		
		0.0741	4.446	266.76		
		0.0735	4.410	264.60		
		0.0731	4.386	263.16		
Nanocrystal Cellulose	2 nm	0.0024	0.141	8.46	$\ln (A_t/A_0)$	7
	4 nm	0.0014	0.086	5.17		
	5 nm	0.0003	0.016	0.94		
PMMA	5 to 15 nm	0.0070	0.420	25.20	$\ln (A_t/A_0)$	8
Colloidal	33 nm	0.0026	0.158	9.47	$\ln (C_t/C_0)$	9
	155 nm	0.0057	0.344	20.63		
$AuCl_4^-$	Sodium squarate	1.5E-06	0.000	0.01		

$AuCl_4^-$	Ascorbic acid	5.5E-05	0.003	0.20	ln (A_t/A_0)	This work
$AuCl_4^-$	Trisodium citrate	6.4E-05	0.004	0.23		
$AuCl_4^-$	Sodium borohydride	8.2E-05	0.005	0.29		
$AuCl_4^-$	Hydrazine	9.8E-04	0.059	3.52		
$AuCl_4^-$	Hydrazine & trisodium citrate	9.6E-04	0.058	3.47		
AuI_4^-	Hydrazine	9.9E-04	0.060	3.57		
AuI_4^-	Hydrazine & Trisodium citrate	1.0E-03	0.060	3.59		

Table S3. Psudeo first order rate constants of literature and this work

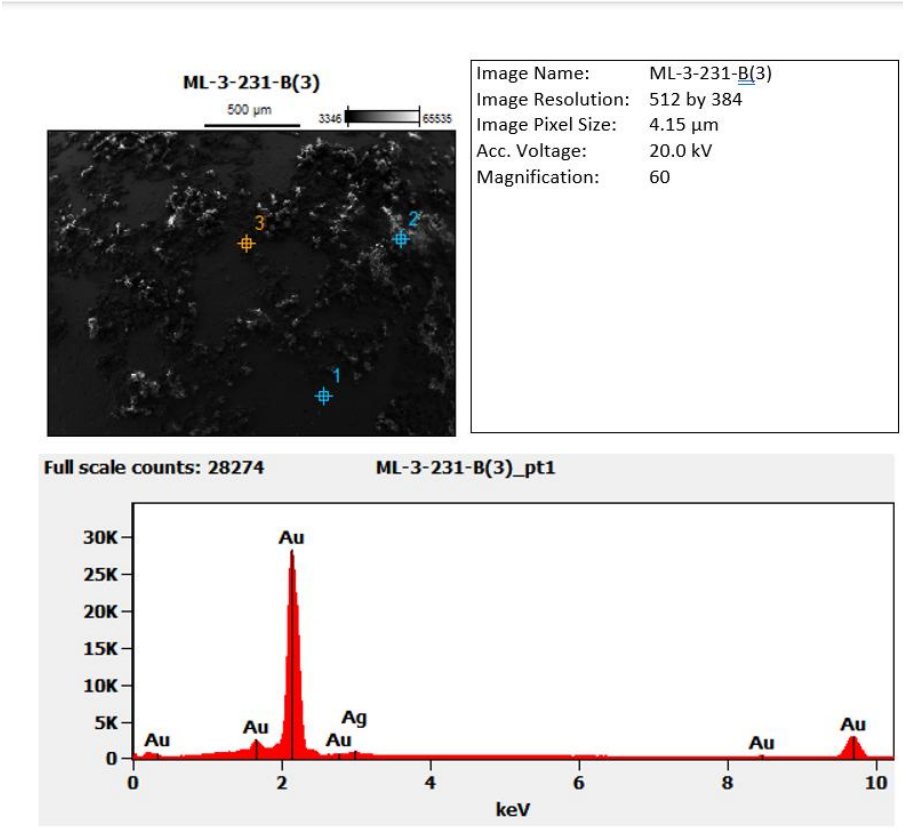

Figure S4. Spot EDS and surface mapping of PGM bead derived from e-waste depicting majority Au and Ag, but unable to determine the presence of Pd

	Average BMLed e-waste (g/kg)	Average g/kg raw e-waste
Sn	**2.84**	**15.18**
Co	**0.00**	**0.00**
Ni	**1.54**	**4.89**
Fe	**10.27**	**72.66**
Al	**4.90**	**27.11**
Mn	**0.30**	**2.35**
Pb	**6.66**	**3.98**
Cr	**2.54**	**1.61**
Zn	**0.23**	**14.38**
Cu	**0.72**	**191.63**
Mg	**0.19**	**1.10**
Au	**0.19**	**0.11**

Table S4. Metal content of e-waste in base-metal leached and raw e-waste

References

1 P. Suchomel, L. Kvitek, R. Prucek, A. Panacek, A. Halder, S. Vajda and R. Zboril, *Sci. Rep.*, 2018, **8**, 4589.

2 T. Ma, W. Yang, S. Liu, H. Zhang and F. Liang, *Catalysts*, 2017, **7**, 38.

3 Md. T. Islam, J. E. Padilla, N. Dominguez, D. C. Alvarado, M. S. Alam, P. Cooke, M. M. J. Tecklenburg and J. C. Noveron, *RSC Adv.*, 2016, **6**, 91185–91191.

4 M. Chen, H. Kang, Y. Gong, J. Guo, H. Zhang and R. Liu, *ACS Appl. Mater. Interfaces*, 2015, **7**, 21717–21726.

5 C. R. Cabreira and F. F. Camilo, *Cellulose*, 2020, **27**, 3919–3929.

6 J. Hwang, A. B. Siddique, Y. J. Kim, H. Lee, J. H. Maeng, Y. Ahn, J. S. Lee, H. S. Kim and H. Lee, *RSC Adv.*, 2018, **8**, 1758–1763.

7 C. Wang, F. Song, X.-L. Wang and Y.-Z. Wang, *Int. J. Biol. Macromol.*, 2022, **209**, 464–471.

8 K. Kuroda, T. Ishida and M. Haruta, *J. Mol. Catal. Chem.*, 2009, **298**, 7–11.

9 Y. S. Seo, E.-Y. Ahn, J. Park, T. Y. Kim, J. E. Hong, K. Kim, Y. Park and Y. Park, *Nanoscale Res. Lett.*, 2017, **12**, 7.